Micromechanical modelling of stress-induced martensitic transformation and detwinning in shape memory alloys

S. Stupkiewicz and H. Petryk

Institute of Fundamental Technological Research, Polish Academy of Sciences

Świętokrzyska 21, 00–049 Warsaw, Poland

e–mail: sstupkie@ippt.gov.pl, hpetryk@ippt.gov.pl

tel. +48 22 8261281 ext. 338, fax +48 22 8269815

Abstract. The paper is concerned with modelling of stress-induced martensitic transformations in single crystals of shape memory alloys. The transformation is assumed to proceed by the formation and growth of parallel martensitic plates within an austenite matrix, as commonly observed in experiments. Phase transition is governed by a time-independent thermodynamic criterion. Martensite variant rearrangement (detwinning) is accounted for in case of internally twinned martensites. The examples illustrate the effect of deformation constraints on the microstructure evolution and overall response. Instability of macroscopically uniform transformation is predicted due to the softening behaviour at the material point scale.

1. INTRODUCTION

Stress-induced martensitic transformation in shape memory alloys (SMA) typically proceeds by the formation and growth of parallel martensitic plates within an austenite matrix. The martensitic plates in a crystal are internally either twinned or faulted which diminishes the transformation strain incompatibility across the coherent interfaces (habit planes) and reduces the related elastic energy. For instance, an austenite β_1 phase in CuAlNi can transform to a twinned γ_1' martensite or internally faulted β_1' martensite, depending on the chemical composition, temperature, as well as on the loading direction and other factors [1, 2]. An internally twinned martensite can undergo further microstructural changes by detwinning, through propagation of mobile interfaces between martensite variants.

This paper deals with the micromechanical modelling of phase transitions in SMA single crystals by using the approach developed recently in [3]. A characteristic feature of this multi-scale model is that under the assumptions of laminated microstructures and separability of scales, it provides a rigorous link between microstructural changes and effective macroscopic properties of the material. The microstructural changes are governed by a threshold condition imposed on local thermodynamic driving forces on transformation fronts. This thermodynamic criterion [4] is conceptually distinct from the minimization of free energy used in a related approach [5], and also differs from the widely adopted Schmid law on account of different elastic properties of the parent and product phases. The present calculations are performed within the small strain framework, however, extension to finite deformations is possible, cf. [6].

The principal aim of the present work is to examine the combined effect of the stress-induced martensitic transformation and detwinning, which was not included in [3]. The results are compared to those without detwinning. The effect of kinematic constraints is also investigated.

2. MODELLING OF EVOLVING LAMINATES

In the approach developed in [3] and followed here, in accord with experimental observations, the stress-induced martensitic transformation in a single crystal is assumed to proceed by the formation of parallel martensitic plates within an austenite matrix. A martensitic plate can either involve only one crystallographic variant of martensite (typically with internal stacking faults) or be a fine mixture of two twin-related

martensite variants. The corresponding basic microstructure is thus a rank-one laminate in the former case and a rank-two laminate in the later case. The microstructure associated with the formation of internally twinned martensite plates is depicted in Fig. 1. A set of combinations of microstructural parameters, such as the habit plane normal $\mathbf{m}$ and the twin plane normal $\mathbf{l}$, can be determined from the crystallographic theory of martensitic transformation [7, 8], at least as the first approximation. The problem of selection of the preferred combination is discussed later. The crystallographic theory provides also the twin fraction λ for which strain compatibility at the austenite-martensite interface holds in the stress-free state. However, in this work the rearrangement of martensite variants during stress-induced transformation is accounted for so that the twin fraction is not constant and transformation strain incompatibility occurs. This is discussed in more detail in Section 4.

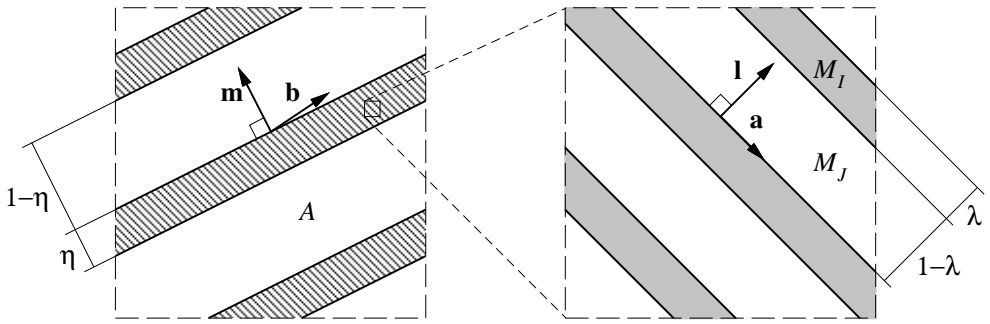

Figure 1. Microstructure (rank-two laminate) associated with the formation of parallel, internally twinned martensite plates (A – austenite, M_I and M_J – martensite variants I and J).

The laminated microstructures are particularly suitable for micromechanical modelling as the micro-macro transition relations can be derived analytically under the assumption that the microstructure is sufficiently fine. In the case of higher-rank laminates this assumption should hold at each scale (the assumption of separability of scales). Consequently, given the microstructure and the local constitutive relations, by applying the averaging rules and interfacial conditions the analytical relationships between local stresses or strains and a macroscopic stress or strain can be determined. The corresponding formulae for the overall (effective) elasticity tensors, stress concentration tensors, and other related quantities, are given in [3] for the case of a simple (rank-one) laminate. Higher-rank laminates are treated accordingly, by applying the micro-macro transition for the simple laminates at each level.

The model is developed in the framework of small strain elasticity with eigenstrains and takes into account different anisotropic elastic properties of austenite and martensite. The corresponding Helmholtz free energy functions of austenite, ϕ_{a}, and of martensite variant I, ϕ_I, are given by

$$\phi_{\mathrm{a}} = \phi_0 + \tfrac{1}{2}\boldsymbol{\varepsilon}\cdot\mathbf{L}_{\mathrm{a}}\boldsymbol{\varepsilon}\,, \quad \phi_I = \phi_0 + \Delta^{\mathrm{am}}\phi_0 + \tfrac{1}{2}(\boldsymbol{\varepsilon}-\boldsymbol{\varepsilon}_I^{\mathrm{t}})\cdot\mathbf{L}_I(\boldsymbol{\varepsilon}-\boldsymbol{\varepsilon}_I^{\mathrm{t}})\,, \tag{1}$$

where $\mathbf{L}_{\mathrm{a}}$, $\mathbf{L}_I$ are the elastic moduli tensors of austenite and of martensite variant I, respectively, $\boldsymbol{\varepsilon}$ is the local total strain, $\boldsymbol{\varepsilon}_I^{\mathrm{t}}$ is the transformation strain of martensite variant I, and $\Delta^{\mathrm{am}}\phi_0$ is the temperature-dependent difference between the free energy densities of martensite and austenite in stress-free states (so called "chemical energy"). Any interfacial energy contribution is neglected.

Quasi-static evolution of the microstructure is assumed to be locally governed by a time-independent thermodynamic criterion of phase transformation, in the form

$$f - f_{\mathrm{c}} \le 0\,, \qquad \dot{s} \ge 0\,, \qquad (f-f_{\mathrm{c}})\dot{s} = 0\,, \qquad f_{\mathrm{c}} \ge 0\,. \tag{2}$$

Here, $\dot{s}$ is the forward rate of thickness of a product phase layer, f is the local thermodynamic driving force (per unit area of the phase transformation front) given in a state of mechanical equilibrium by

$$f = \boldsymbol{\sigma}\cdot\Delta\boldsymbol{\varepsilon} - \Delta\phi\,, \tag{3}$$

where the stress $\boldsymbol{\sigma}$ can be taken from any side of the front and $\Delta\boldsymbol{\varepsilon}$ and $\Delta\phi$ are the forward jumps in the strain and in the Helmholtz free energy density, respectively. A threshold value f_{c} for the driving force in (2) can in general be state dependent and must be nonnegative due to the requirement of nonnegative dissipation. A complete set of the formulae that define the model along with references to the related literature can be found in [3].

3. UNTWINNED MARTENSITE: EVOLVING RANK-ONE LAMINATE

Consider first the case when the product phase does not undergo any internal microstructural changes as the transformation proceeds on the macroscopic level, which is possible, for example, for internally faulted (untwinned) 18R martensites in Cu-based alloys.

The crystallographic theory in [9] (being the specification of the general theory [8] for the case of untwinned martensites) provides the microstructural parameters for all possible martensite plates (habit plane variants), namely the index of the crystallographic (lattice correspondence) variant, the habit plane normal vector $\mathbf{m}$ and the shape strain vector $\mathbf{b}$. In the geometrically linear approximation [10], the related transformation strain of the martensite plate is given by $\boldsymbol{\varepsilon}^{\mathrm{t}} = \frac{1}{2}(\mathbf{m}\otimes\mathbf{b} + \mathbf{b}\otimes\mathbf{m})$, where $\mathbf{m}$ and $\mathbf{b}$ slightly differ, cf. [11], from those in [9].

Prediction of the microstructural rearrangements in the material for a specified loading program involves two basic steps: selection of the *preferred* habit plane variant and determination of the volume fraction of martensite plates with that habit plane in the course of transformation. Both steps are performed with the help of the transformation criterion (2), where $\dot{s}$ can be replaced with the forward rate $\dot{\eta}$ of the volume fraction of martensite. The preferred habit plane variant is selected as the first one for which the transformation criterion is satisfied for $\eta = 0$ and $\dot{\eta} > 0$ at the smallest value of a monotonically increasing control parameter, e.g. overall axial strain. Once the habit plane variant is chosen, the volume fraction of martensite η is the only unknown microstructural parameter that can be determined from the transformation criterion.

A detailed description of the model and its application for the cubic-to-orthorhombic ($\beta_1 \rightarrow \gamma_1'$) transformation in CuAlNi can be found in [3]. In that paper, an additional assumption was used that internally twinned plates of γ_1' martensite did not undergo detwinning. Here, the cubic-to-monoclinic transformation in CuZnAl is examined which produces internally faulted 18R martensite, so that detwinning is irrelevant. Figure 2 shows the predicted macroscopic stress-strain response in isothermal uniaxial tension of a single crystal for three loading directions A, D and F, selected from those shown in the unit stereographic triangle. The crystallographic lattice parameters that define the transformation strain are taken from [12], and the elastic constants of austenite and martensite single crystals from [13, 14]. The diagrams in Fig. 2 correspond to $\Delta^{\mathrm{am}}\phi_0 = 7.5$ MJ/m^3 and $f_{\mathrm{c}} = 0.5$ MJ/m^3.

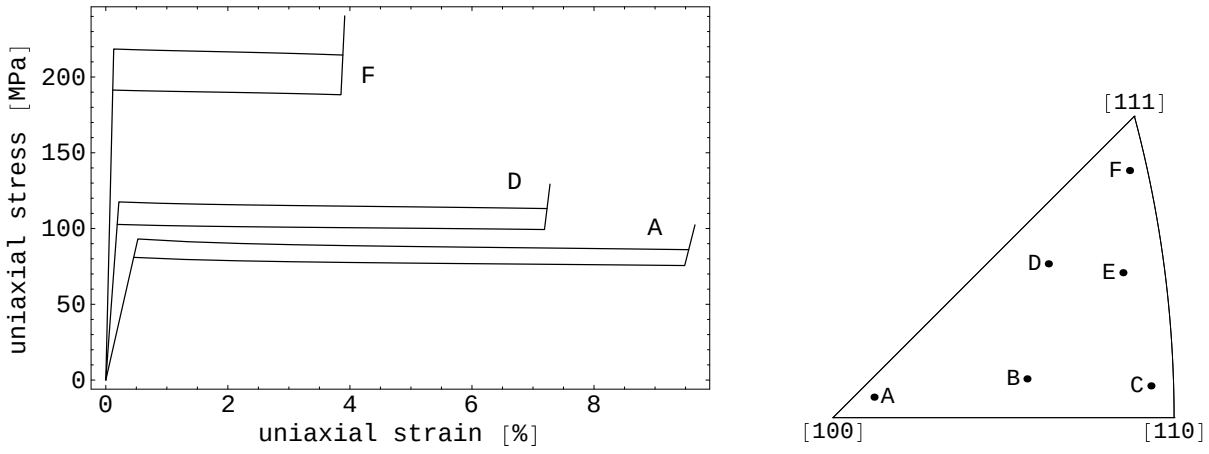

Figure 2. Uniaxial tension of CuZnAl single crystal undergoing cubic-to-monoclinic transformation (18R martensite).

The model accounts for the difference in elastic properties of both phases and for the related redistribution of local stresses in layers. As discussed in [3], this leads to a slightly negative tangent modulus accompanying the progressive transformation. Also the predicted transformation stresses are somewhat different from those predicted by the Schmid law.

4. TRANSFORMATION AND DETWINNING: EVOLVING RANK-TWO LAMINATE

4.1 Mobile twin interfaces

Consider now the case when martensite plates have an internal microstructure being a fine mixture of two twin-related martensite variants, cf. Fig. 1. Contrary to internally faulted martensites, the internal microstructure can change during transformation due to migration of twin boundaries. This is associated with martensite variant rearrangement (detwinning) and with the variation of effective properties (i.e., elastic moduli and transformation strain) of a martensite plate.

A mobile twinning plane can be considered as a phase transformation front but with no chemical energy associated with martensite variant rearrangement, cf. $(1)_2$. Furthermore, below we assume for simplicity that the critical driving force for propagation of a twinning plane is equal to zero. This implies that there is no dissipation directly associated with detwinning. This assumption can easily be relaxed to allow some (typically small) dissipation related to propagation of twin interfaces, which has not been found to change the results significantly.

As discussed above, the parallel, internally twinned martensite plates form an evolving rank-two laminate. This microstructure is fully characterised once the following parameters are determined: martensite variant pair (I, J), the twinning plane and habit plane normal vectors $\mathbf{l}$ and $\mathbf{m}$, respectively, the twin fraction λ and the volume fraction of martensite η, cf. Fig. 1.

Consider the forward transformation from austenite to martensite and assume first that the variant pair (I, J) and vectors $\mathbf{l}$ and $\mathbf{m}$ are known. For given external loading conditions, the remaining two microstructural parameters λ and η can be found from two equations: the transformation criterion at the twinning plane, $f^{JI} = 0$, and the transformation criterion at the austenite-twinned martensite plate interface, $f^{\mathrm{am}} = f^{\mathrm{am}}_{\mathrm{c}}$. Here f^{JI} and f^{am} denote the respective thermodynamic driving forces and $f^{\mathrm{am}}_{\mathrm{c}}$ is the critical driving force for the austenite-to-martensite transformation. The local stresses and strains necessary to compute the driving forces f^{JI} and f^{am} follow from the micro-macro transition formulae for the rank-two laminate at hand.

The variant pair (I, J) and vectors $\mathbf{l}$ and $\mathbf{m}$ are selected by applying the above procedure at $\eta = 0$, i.e., at the onset of transformation, for all microstructures (i.e. all possible martensite plates) predicted by the crystallographic theory. The preferred martensite plate is then chosen for which the transformation is initiated first for the prescribed loading program, just like in the case of untwinned martensites, Section 3.

4.2 Uniaxial tension of CuAlNi single crystal

As an example, consider isothermal uniaxial tension of a CuAlNi single crystal undergoing a $\beta_1 \rightarrow \gamma_1'$ (cubic-to-orthorhombic) transformation. The loading program is specified by prescribing the macroscopic axial strain jointly with the condition that all *macroscopic* (but not local) stress components, except the macroscopic axial stress, vanish. The macroscopic stress is thus expressed by $\bar{\boldsymbol{\sigma}} = \sigma_{\mathrm{u}} \mathbf{t} \otimes \mathbf{t}$, where $\mathbf{t}$ is a unit vector aligned with the tension axis. The needed material parameters (elastic constants and lattice parameters) are given in [3], where the same example was analysed but with the simplifying assumption of constant twin fraction λ, i.e., according to the scheme outlined in Section 3. That assumption is now dropped.

The overall stress-strain response and the evolution of microstructural parameters predicted for the stress-induced transformation are shown in Fig. 3. The tension axis is specified by $\mathbf{t} = [0.925, 0.380, 0.]$, with respect to the cubic basis of austenite. The dashed lines in Fig. 3 correspond to the case of constant

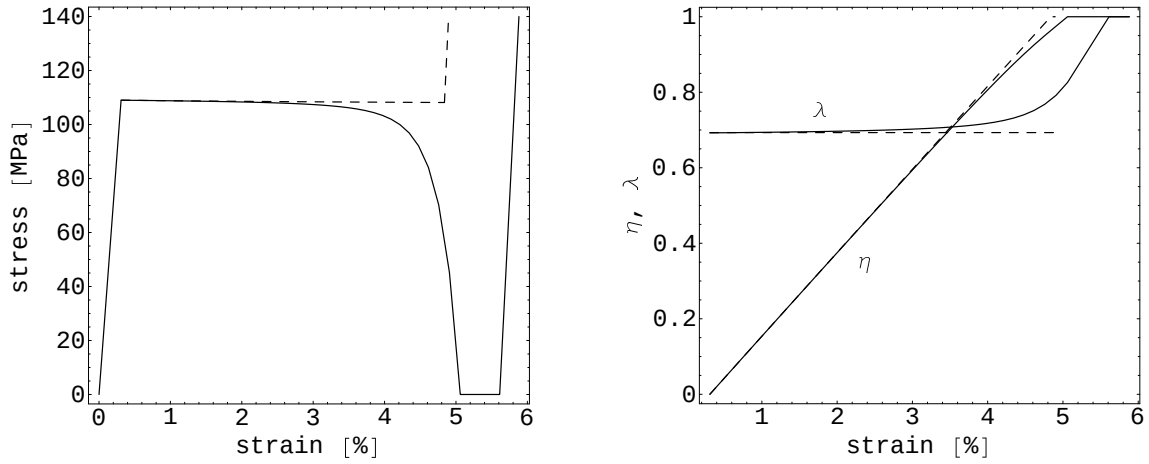

(a) (b)

Figure 3. Uniaxial tension of CuAlNi single crystal undergoing $\beta_1 \rightarrow \gamma_1'$ transformation: (a) stress-strain diagram and (b) evolution of twin fraction λ and volume fraction η of martensite. Solid lines denote the case of mobile twinning planes and dashed lines correspond to the fixed twin fraction λ.

twin fraction λ, equal to that predicted by the crystallographic theory. Only the forward transformation from austenite to martensite is analysed.

The predicted effect of detwinning on the overall response of the material is clearly visible in Fig. 3. The volume fraction λ of one martensite variant within the plate grows substantially at the expense of the other variant, Fig. 3(b), near the end of transformation. This leads to a strongly negative slope of the macroscopic stress-strain diagram with a significant drop of the macroscopic stress, Fig. 3(a). At the instant when austenite disappears ($\eta = 1$) the overall stress falls to zero and further detwinning proceeds at zero stress until the less favorable variant disappears ($\lambda = 1$). This is followed by elastic loading of the remaining single variant of martensite. Qualitatively similar results have also been obtained recently in [5] where a tetragonal product phase and uniform isotropic elastic properties were assumed.

To explain this somewhat surprising effect we note that as austenite disappears, the average stress in a martensite plate tends to the overall stress $\bar{\boldsymbol{\sigma}}$. The driving force f^{JI} can thus be expressed in the limit $\eta = 1$ in terms of $\bar{\boldsymbol{\sigma}}$ as a sum of the leading term $\bar{\boldsymbol{\sigma}} \cdot (\boldsymbol{\varepsilon}_I^{\mathrm{t}} - \boldsymbol{\varepsilon}_J^{\mathrm{t}}) = \sigma_u \mathbf{t} \cdot (\boldsymbol{\varepsilon}_I^{\mathrm{t}} - \boldsymbol{\varepsilon}_J^{\mathrm{t}})\mathbf{t}$ and a quadratic correction term due to the mutual rotation of the elastic compliance tensors in martensite variants, in analogy to the formula (36) in [3]. In the circumstances met in the calculations above, the leading term with fixed $\mathbf{t} \cdot (\boldsymbol{\varepsilon}_I^{\mathrm{t}} - \boldsymbol{\varepsilon}_J^{\mathrm{t}})\mathbf{t} \neq 0$ cannot be compensated by the correction term to produce $f^{JI} = 0$, unless $\sigma_u = 0$ in the limit. Therefore, the overall stress must decrease to zero as austenite disappears; further variant rearrangement proceeds likewise at zero stress. The stress would not fall exactly to zero if a positive threshold value for f^{JI} was assumed, $f_{\mathrm{c}}^{JI} > 0$, but the general behaviour would not change significantly for physically realistic twinning-related dissipation (proportional to f_{c}^{JI}).

The behaviour illustrated in Fig. 3(a) by the solid line seems to be not in accord with typical stress-strain diagrams obtained from experimental tests on SMA specimens. However, it must be emphasized that the micromechanical model predicts the material behaviour under the assumption of development of a uniformly laminated microstructure within a material element. The transition from the material element scale to the scale of a single-crystal specimen or a grain in a polycrystal requires additional analysis, to be presented elsewhere. Here, we restrict ourselves to sketch two hypothetical responses of a single-crystal specimen, cf. Fig. 4. The expected instability of macroscopically unifrom transformation can lead to localization of transformation zones. A negative tangent modulus for the material allows the transformation to proceed locally while the remaining part of the specimen undergoes elastic unloading. Moreover, the transformation may even be locally completed in a dynamic manner at fixed overall elongation Δl, corresponding to a local jump indicated schematically in Fig. 4 by a dashed line. If such transformation takes place repeatedly in finite zones then the resulting force–elongation (P–Δl) diagram for the specimen may

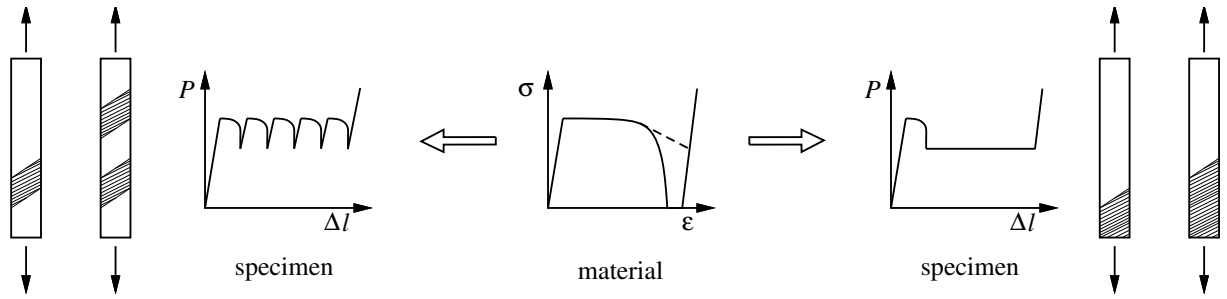

Figure 4. Two hypothetical responses of a specimen with localized transformation zones.

have the form sketched on the left-hand side of Fig. 4. Alternatively, smooth expansion of the fully transformed zone may lead to a diagram of the form sketched on the right-hand side of Fig. 4. Experimental stress-strain diagrams of both kinds have been reported in the literature, cf. [1, 2, 15]. The instability phenomena are thus expected to play a crucial role in the microstructure evolution and overall behaviour of SMA specimens, which will be analysed in more detail in a separate paper.

4.3 Constrained deformation under tension

In the case of uniaxial tension studied in Section 4.2 the only non-zero component of the overall stress tensor $\bar{\boldsymbol{\sigma}}$ is the axial component $(\bar{\boldsymbol{\sigma}}\mathbf{t})\cdot\mathbf{t}$, equal to σ'_{11} if x'_1-axis is aligned with $\mathbf{t}$. This implies that the deformation is completely free in a sense that all the complementary components of the overall strain tensor $\bar{\boldsymbol{\varepsilon}}$ can take arbitrary values. This is a very idealized situation, especially for a grain in a polycrystalline material due to the constraints imposed by neighbouring grains, but also for an anisotropic tensile specimen with constrained grips. The effect of constrained deformation is therefore investigated in this section.

In order to study the effects of constrained deformation on transformation and detwinning, assume that in addition to tensile loading the following constraint is imposed on the overall strain

$$(\bar{\boldsymbol{\varepsilon}}\mathbf{t})\cdot\mathbf{s}=0 \qquad \text{or} \qquad \bar{\varepsilon}'_{12}=0\,, \tag{4}$$

where a unit vector $\mathbf{s}$ aligned with x'_2-axis is perpendicular to the tensile loading direction $\mathbf{t}$, i.e., $\mathbf{t}\cdot\mathbf{s}=0$. Clearly, the respective overall stress component $(\bar{\boldsymbol{\sigma}}\mathbf{t})\cdot\mathbf{s}=\bar{\sigma}'_{12}$ is not equal to zero in general. The constraint (4) approximately applies to a thin sheet-like specimen (with $\mathbf{s}$ and x'_2-axis lying within the sheet plane) subjected to tensile loading with the grips constrained laterally.

The results obtained for two specific loading conditions are shown in Fig. 5. The tension axis is assumed as that in Section 4.2 ($\mathbf{t}=[0.925, 0.380, 0.]$), and the constraint (4) is applied corresponding to two sheet orientations $\mathbf{s}=[-0.380, 0.925, 0.]$ (case A) or $\mathbf{s}=[-0.190, 0.463, 0.866]$ (case B), mutually rotated by 60°. The resulting stress-strain diagrams are shown by the solid lines in Fig. 5, while the dashed lines correspond to the case of a fixed twin fraction λ. Comparison with Fig. 3(a) shows that the presence of constraint (4) changes the material response substantially.

According to the assumption of the model, the twin fraction λ varies so that the driving force on the twinning plane be equal to zero. In case A the twin fraction of the most favorable martensite variant increases as the transformation proceeds from $\lambda=0.711$ at $\eta=0$ to $\lambda=0.774$ at $\eta=1$, cf. Fig. 6. Due to partial detwinning the pseudoelastic strain at $\eta=1$ is larger as compared to the case of fixed twin fraction, cf. Fig. 5(a). Further loading of the twinned martensite (after transformation is completed) is accompanied by additional detwinning with the twin fraction reaching $\lambda=0.8$ at the tensile stress of $201\,\mathrm{MPa}$. For comparison, the purely elastic response of the twinned martensite with the twin fraction fixed at $\lambda=0.774$ is marked in Fig. 5(a) by the dotted line. Clearly, detwinning provides additional strain so that the response is more compliant. The values of the effective elastic and tangent stiffness moduli are given in Table 1.

A qualitatively different behaviour is predicted in case B. The twin fraction of the most favorable variant *decreases* during progressive transformation, Fig. 6. This results in a hardening stress-strain response. Also the pseudoelastic strain is somewhat smaller than in the case of constant twin fraction, cf. Fig. 5(b).

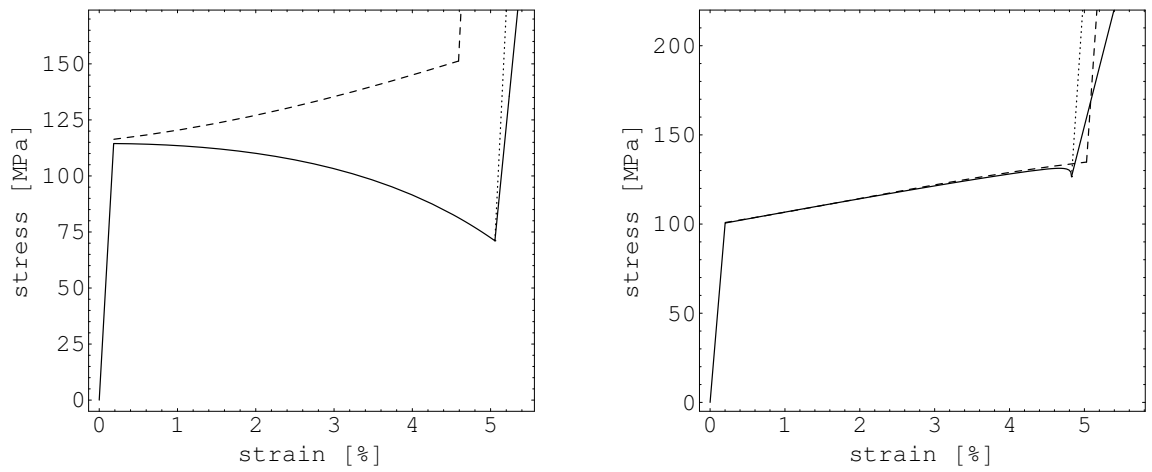

Figure 5. Constrained tension of CuAlNi single crystal undergoing $\beta_1 \rightarrow \gamma_1'$ transformation. Stress-strain diagrams for $\mathbf{t} = [0.925, 0.380, 0.]$ and (a) $\mathbf{s} = [-0.380, 0.925, 0.]$, (b) $\mathbf{s} = [-0.190, 0.463, 0.866]$. Solid lines denote the case of mobile twinning planes and dashed lines correspond to a fixed twin fraction λ.

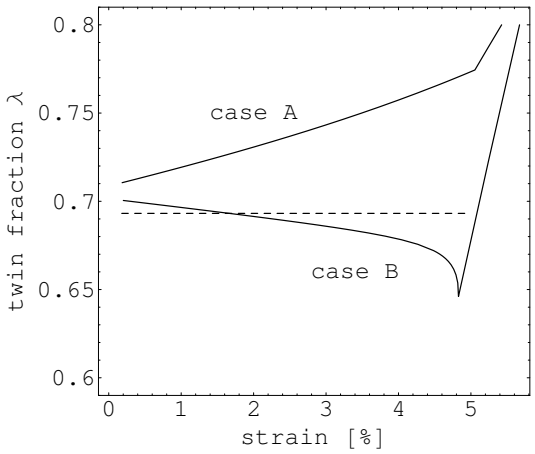

Figure 6. Constrained tension of CuAlNi single crystal: variation of twin fraction λ.

However, once the transformation is completed, the elastic loading of martensite is associated with the growth of the favorable variant at the expense of the other one. The detwinning-related reduction of the effective tangent stiffness modulus is even more pronounced than in case A, cf. Table 1.

5. Concluding remarks

The micromechanical model [3] of evolving laminated microstructures has been used to investigate the combined effect of the stress-induced martensitic transformation and detwinning in single crystals of shape memory alloys with internally twinned martensites. Evolution of the corresponding rank-two laminate has been examined with the help of a time-independent thermodynamic criterion of phase transformation and for a negligible critical driving force on mobile interfaces between twin-related martensite variants.

By the example of a CuAlNi single crystal undergoing the $\beta_1 \rightarrow \gamma_1'$ transformation, it has been shown that detwinning leads to a significant softening behaviour visualized in the macroscopic stress-strain diagram for a representative element of the material. In the case of unconstrained deformation in uniaxial tension, the stress can even drop to zero as austenite disappears. This is related to instability of macroscopically uniform transformation which can manifest itself in the creation of localized transformation zones. This makes the stress-strain diagrams for a material element and for the specimen fundamentally distinct.

The effect of constrained deformation on the evolution of microstructure and on the macroscopic re-

Table 1. Effect of detwinning on the effective tangent stiffness modulus in constrained tension of CuAlNi crystal.

	case A	case B
martensite, detwinning	35.3 GPa	17.5 GPa
martensite, no detwinning	70.6 GPa	62.6 GPa
austenite	62.0 GPa	50.0 GPa

sponse has been illustrated by the example of tension with constrained shear. It has been shown that the difference in orientation of the shear constraint may lead to different detwinning effects, e.g., to the increase or decrease of the volume fraction of the favorable martensite variant in twinned martensite plates.

On completing the austenite to martensite transformation, detwinning can still take place and influence the apparent stiffness of the martensite. Detwinning has been found to reduce significantly the effective tangent stiffness modulus of the twinned martensite. Hence, care is needed when interpreting apparent Young's modulus of martensite as representing its purely elastic stiffness.

Acknowledgement

This work has been partially supported by the State Committee for Scientific Research (KBN) in Poland through Grant No. 8 T07A 044 20.

References

[1] Otsuka, K., Wayman, C.M., Nakai, K., Sakamoto, H., Shimizu, K., *Acta Metall.* **24** (1976) 207–226.
[2] Novák, V., Šittner, P., Zárubová, N., *Mater. Sci. Eng.* **A234–236** (1997) 414–417.
[3] Stupkiewicz, S., Petryk, H., *J. Mech. Phys. Solids* **50** (2002) 2303–2331.
[4] Rice, J.R., In: *Constitutive Equations in Plasticity*, edited by A.S. Argon (MIT Press, Cambridge, Mass., 1975) pp. 23–79.
[5] Roytburd, A.L., Slutsker, J., *J. Mech. Phys. Solids* **49** (2001) 1795–1822.
[6] Petryk, H., *J. Mech. Phys. Solids* **46** (1998) 873–894.
[7] Wechsler, M.S., Lieberman, D.S., Read T.A., *Trans. AIME J. Metals* **197** (1953) 1503–1515.
[8] Ball, J.M., James, R.D., *Arch. Ration. Mech. An.* **100**, (1987) 13–50.
[9] Hane, K.F., *J. Mech. Phys. Solids* **47** (1999) 1917–1939.
[10] Bhattacharya, K., *Continuum Mech. Thermodyn.* **5** (1993) 205–242.
[11] Stupkiewicz, S., *Eur. J. Mech. A/Solids* (to appear).
[12] Chakravorty, S., Wayman, C.M., *Acta Metall.* **25** (1977) 989–1000.
[13] Guenin, G., Morin, M., Gobin, P.F., Dejonghe, W., Delaey, L., *Scripta Metall.* **11** (1977) 1071–1075.
[14] Rodriguez, P.L., Lovey, F.C., Guenin, G., Pelegrina, J.L., Sade, M., Morin, M., *Acta Metall. Mater.* **41** (1993) 3307–3310.
[15] Zhang, X.Y., Sun, Q.P., Yu, S.W., *J. Mech. Phys. Solids* **48** (2000) 2163–2182.